Pergamon

Bioorganic & Medicinal Chemistry 7 (1999) 143–151

BIOORGANIC & MEDICINAL CHEMISTRY

C-Terminal Capping Motifs in Model Helical Peptides

Neville R. Kallenbach* and Youxiang Gong†

Department of Chemistry, New York University, New York, NY 10003, USA

Received 20 April 1998; accepted 12 October 1998

Abstract—Solution structures of a series of consensus sequence peptides with N- and C-terminal capping interactions have been determined by 2-D nuclear magnetic resonance spectroscopy and a simulated annealing strategy. All peptides are found to be stabilized by a hydrophobic interaction and a capping box structure (SXXE) at the N-terminus whereas several different capping motifs are discerned near the peptide C-terminus. Among these, the asparagine side chain-backbone main chain (i, i-4) capping structure is most stabilizing and highly populated in the simulated annealing calculation. A glycine α_L capping motif stabilizes the peptide terminus, which otherwise tends to fray, but this is occupied only a fraction of the time in the trial structures determined. Our experimental search over several models for a second type of C-terminal capping structure, the so-called 'Schellman motif', which is seen in native proteins, is unsuccessful, indicating this structural element contributes less to oligopeptide stability in solution and most probably populates only transiently.

Introduction

The α helix is one of a small number of fundamental structural motifs in the native structure of proteins.[1] Helix occurs frequently in the native states of globular proteins and fibrous proteins—more than 25% of the residues in globular proteins of known structure have φ and ψ angles within the range of helical conformation.[2] Inspection of native protein structures suggests a variety of plausible interactions that are capable of stabilizing helical structure.[3] Pauling[1] initially attributed the stability of the alpha helix to strongly favorable H-bonding in the main chain, which he estimated would provide more than 5 kcal/mol. Subsequently it has been shown that the situation is not so simple, and the balance of stabilizing and destabilizing interactions in a helix is much more delicate. Some of the contributing factors include the helix propagation constant or helix propensity of each side chain,[4–6] which takes into account the intrinsic conformational restriction experienced by forcing a side chain into helix;[7] electrostatic interactions between charged side chains and charged side chains of the same or opposite sign, polar side chains, and/or the helix dipole,[8–10] and packing interactions between long side chains spaced appropriately along a helix.[11]

The mean length of the helices in globular proteins is short—about 12 amino acids.[12] In such short helices, four peptide groups at the N- and the C-termini of a helix are unable to satisfy the peptide H-bonding potential via H-bonding to the main chain itself.[12,13] Instead, polar side chains at the N- and C-termini can interact with peptide groups at the ends of the helix to replace at least part of the missing backbone H-bonding potential.[13–15] The structure at the ends of helices is important in nucleating helix, and the principles underlying both N- and C-terminal capping need to be understood, since these exist in protein helices as well as model peptides.

One classical N-terminal motif is the capping 'box' identified first by Harper and Rose.[16] This structure involves two complementary side chain–main chain H-bonding interactions, one between the Ser side chain and the amide of Glu, the second the side chain of Glu and the amide of Ser. This structure characterizes the N-termini of each of the peptides of this study as well as many helices in proteins, directing the N-terminus of the molecule in a direction perpendicular to the helix axis.[17] Bulky nonpolar groups at the N-terminus have also been identified as a factor contributing to N-terminal helix capping interactions.[11] This has been referred to as a hydrophobic staple, although hydrophobic interactions may only account for part of the effect.[18] We are here concerned with the diversity of structures at the C-termini in this group of peptides, as well as refinement of the overall structure in the molecules to clarify the status of the N-terminus.

The presence of an unusual type of H-bond at the C-terminus of the H-helix in myoglobin was first reported by Watson.[19] Subsequently C. Schellman[20] reported that about one-third of helices in proteins end in a residue with a left-handed (α_L) conformation, having

*Corresponding author. Tel.: +1 (212) 998 8757; fax: +1 (212) 260 7905; e-mail: kallnbch@is.nyu.edu

†R&D Center, Boehringer–Ingelheim Pharmaceuticals, Inc., Ridgefield, CT 06877.

0968-0896/99/$ - see front matter
PII: S0968-0896(98)00231-4

positive ϕ,ψ angles favored by the presence of a Gly residue. Due to the extended freedom of its backbone, glycine can readily adopt an α_L conformation, satisfying two successive backbone CO groups while turning the axis of the chain in a direction that terminates the helix, allowing a large exposure of the main chain CO groups.[12]

Helices terminating in Gly have been classified into two major structural motifs.[21] The Schellman motif has a distinctive, doubly hydrogen bonded pattern between backbone partners, consisting of 6→1, 5→2 hydrogen bonds between the NH at position i + 1 and the CO at position i-4 and between the NH at position i (Gly) and CO at position i-3, respectively. The second Gly α_L motif consists of a 5→1 hydrogen bond between the NH at i (the Gly residue) and a CO at i-4 (Fig. 1). According to Aurora et al.,[21] each of these structural motifs has two 'facets'—one helical and the other not. The helical facet rigidifies the final helical turn, by hydrogen bonding back to the main chain CO, whereas the other facet terminates the helix and directs the polypeptide chain along a new trajectory.

In order to clarify the role of C-capping interactions, we have carried out a detailed analysis of the solution structures of a series of peptides with consensus sequence. These peptides incorporate one of the

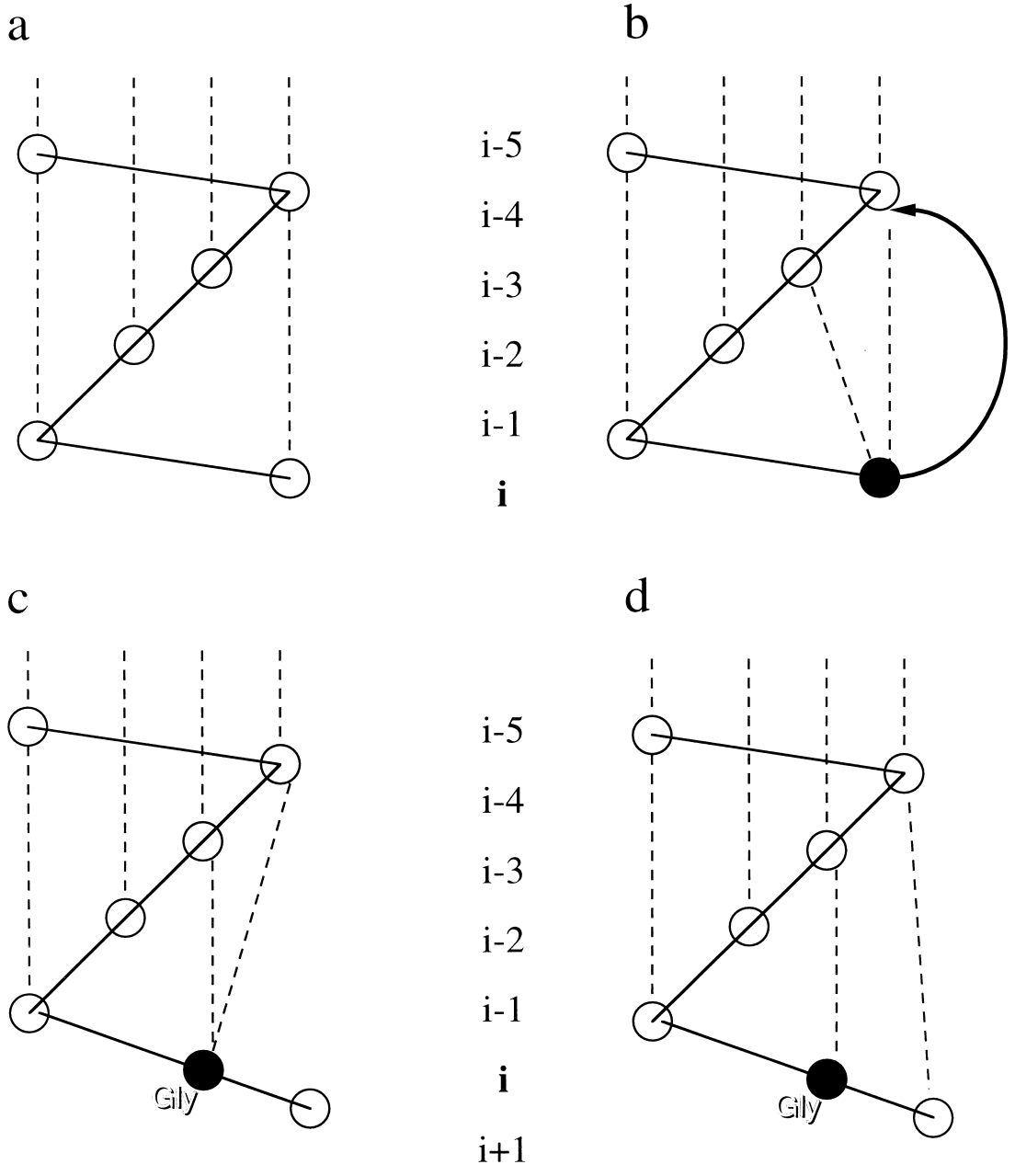

Figure 1. Schematic diagrams illustrating C-terminal structures. The backbones and hydrogen bonds are shown by solid line and dashed lines, respectively: (a) helix continuation; (b) side chain–main chain cap with the bold line showing side chain–main chain H-bond; (c) glycine α_L cap; and (d) Schellman motif.

statistically most frequent amino acids at each position in the chain, derived from the survey by Richardson and Richardson.[12] Substitutions in these peptides have revealed that distinctive capping structural patterns arise in sequences that show high helicity. One exceptionally strong interaction involves Asn near the C-terminus,[22] interacting with the main chain three residues away; this sequence produced the highest helicity among dozens of guest substituents investigated in this series. A Gly α_L capping structure was also seen to stabilize the peptide C-terminus significantly, but the structure is occupied only a fraction of the time.[17] The postulated 'Schellman motif' is not seen in any member of this series of peptides, indicating that it contributes less to the oligopeptide stability in solution and most probably populates only transiently.

Results

Peptide design rationale

The series of peptides of this study consist of 20mers, based on the parental sequence:

YMSEDELKAAEAAFKRHGPT

which includes the most frequently occurring side chains in the helices of globular proteins near the N- and C-termini,[12] spaced with the insert AAEAA to block N- and C-terminal interactions and ensure helix nucleation.[15] A series of guest substitutions in this host helix have been synthesized and studied,[15,17,22] including variants containing multiple substitutions in the middle of the chain, at the N-terminus and at the C-terminus. These allow comparison of the stability and structure of chains with fixed N-terminal motifs, and fixed C-terminal motifs. Table 1 illustrates the group of peptide sequences that define alternative states of the C-terminus, fixing the N-terminus in a classical SXXE capping box. The Met2 residue folds across one face of the helix, linking with Leu7.[17] The C-terminal position in these peptides is residue 18, the Pro and Thr residues corresponding to extrahelical structure in the protein sequences these sequences are taken from. The presence of Pro at position 20 can favor capping also,[17] via packing against nonpolar side chains towards the N-terminus-Phe14 in our case. The presence of Pro19 has been observed to influence the action of the adjacent Gly residue.[22] That is, the α_L configuration of Gly18 allows the next peptide group in the chain to interact—however, this is precluded by presence of Pro19. Polar side chains were introduced at position 18 to establish the possibility of a capping process involving side chain–main chain H-bonding as in the case of the N-terminus. Such an interaction was detected for Asn18, which shows the highest helicity among the variants listed in Table 1. The remaining structures were determined precisely to define the role of Gly18 in C-terminal capping.

CD spectroscopy

The circular dichroism spectra, taken at a peptide concentration of 34 μM, 4 °C and pH 6.0, with two minima at 222 and 208 nm and a maximum at 195 nm indicate a high population of helical conformation for all peptides (data not shown).[23,24] This conclusion is supported by the data from two-dimensional nuclear magnetic resonance (NMR) experiments. We calculated the percent helicity using $[-[\theta]_{obsd}/22{,}000]\times 100\%$[23] and the results are given in Table 1. It should be pointed out that the value of 47% for GWS is highly inaccurate due to the presence of a tryptophan residue at position 18. We corrected for the effect of Trp as described in Chakrabartty et al.[25] by utilizing $-[\theta]_{obsd}/[40{,}000(n-4)/n-2300]$ as the percent helical content. The thermal transitions of these peptides are noncooperative and do not allow evaluation of thermodynamic parameters.

NMR spectroscopy

We have analyzed all peptides listed in Table 1 by 2-dimensional nuclear magnetic resonance (NMR). All complete assignments of proton chemical shifts of peptides were achieved employing Wüthrich's strategy,[26] which combines COSY-type spectra with NOESY spectra. The amino acid spin systems were identified by the through bond coupling network of the DQF-COSY and TOCSY experiments collected in 90%/10% H_2O/D_2O at pH 6.0. The fingerprint region of TOCSY spectrum for NPT is shown in Figure 2. The sequence specific assignments of amino acids were further carried out by through-space NOE connectivities of the NOESY and ROESY experiments. The chemical shift assignments for peptide NPT are summarized in Table 2. The

Table 1 Studied peptide sequences and relative helical content

Peptides	Sequences[a]																				$-[\theta]_{222}$[b]	F(%)
Parent S3	Y	M	S	E	D	E	L	K	A	A	E	A	A	F	K	R	H	G	P	T	16,000	50
APT	Y	M	S	E	D	E	L	K	A	A	E	A	A	F	K	R	H	A	P	T	17,400	54
NPT	Y	M	S	E	D	E	L	K	A	A	E	A	A	F	K	R	H	N	P	T	20,000	63
QPT	Y	M	S	E	D	E	L	K	A	A	E	A	A	F	K	R	H	Q	P	T	17,920	56
SPT	Y	M	S	E	D	E	L	K	A	A	E	A	A	F	K	R	H	S	P	T	17,400	54
GVP	Y	M	S	E	D	E	L	K	A	A	E	A	A	F	K	R	H	G	V	P	18,340	57
GIS	Y	M	S	E	D	E	L	K	A	A	E	A	A	F	K	R	H	G	I	S	17,400	54
GWS	Y	M	S	E	D	E	L	K	A	A	E	A	A	F	K	R	H	G	W	S	16,570	52, 48[c]

[a]All the peptides in this table were acetylated at the N-terminus and amidated at the C-terminus, as described previously.[15,22]
[b]$-[\theta]_{222}$ is the mean residue ellipticity (degree cm^2 dmol^{-1}) at 222 nm, 4 °C, pH 6.0 $F=[-[\theta]_{obsd}/40{,}000(n-4)/n]\times 100\%$ = percent helix content.[23]
[c]52% is calculated as if aromatic effect of Trp is not present whereas 48% is the corrected value.

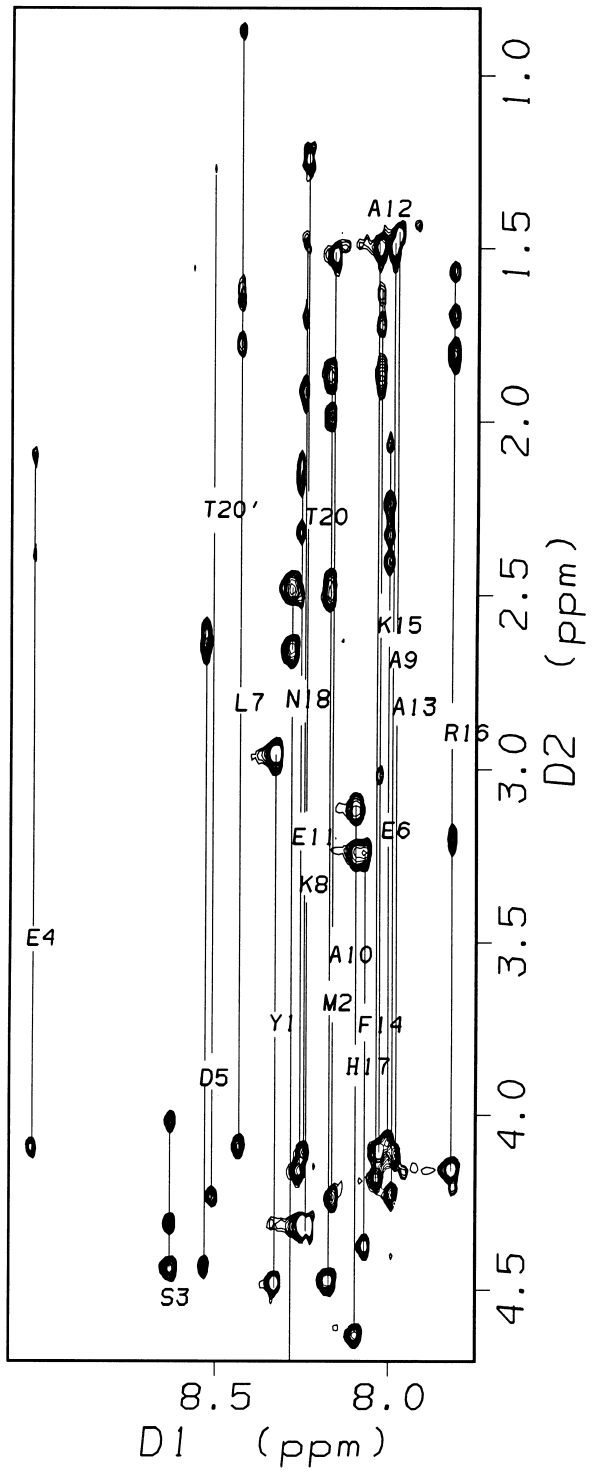

Figure 2. Fingerprint region of the TOCSY spectrum of NPT at 10 °C. Individual spin systems are identified by standard one-letter symbols for the amino acids and the sequential numbers in the sequence. Two sets of cross peaks can be seen for Thr20 due to the *trans–cis* conformation of Pro19 residue. The amide of Asn18 is not shown here due to the high drawing contour level used.

$^3J_{HN\alpha}$ coupling constants shown in Table 2 are values corrected for line shape effects using Wüthrich's method.[26]

Figures 3 and 4 show the $^{\alpha}$H–NH region of peptide GIS and NH–NH region of GWS of NOESY spectra with mixing time 200 ms in H_2O at pH 6.0 and 10 °C. A clear pattern of cross peaks linking neighboring amide protons from N-termini (from Met2 for all peptides) to C-termini (to residue 17 for most of the peptides) can be detected. Many of the intermediate-range cross peaks can be assigned unambiguously too, indicating that all peptides have the same N-terminal capping structures and central helical conformation as those in GVP.[17] There are differences in the C-terminal NOE connectivities. A crosspeak between the side chain NH_2 of Asn18 and $^{\alpha}$H of Phe14 was observed in the NOESY spectrum,[27] indicative of presence of a side-chain backbone H-bonding. The NOE pattern and solution structures from NOE constraints have revealed a Gly α_L motif in GVP peptide, in which the Gly takes a positive ϕ angle of 98.4°.[17] A stretch of adjacent NH–NH NOE peaks from Met2 to Trp19 was observed for GWS (Fig. 4), evidencing a helix continuation near the C-terminus. In peptides GVP, GIS and GWS no side chain–side chain interaction between the side chain of Val/Ile/Trp (i + 1) and the aromatic ring of Phe (i-4), characteristic of C-terminal 'Schellman motif',[20,21] was observed in the present study.

Simulated annealing results

An overview of the restraints employed in the simulated annealing calculations and the violations of the final solution structures of NPT are presented in Table 3. Minimized local RMSD values calculated for C′, C^{α} and N for all possible combinations of pairs of the 10 structures (45 combinations total) reveal a well-defined backbone structure from residue Ser3 to Asn18 (all RMSD < 0.8 Å, center helix Leu7–Ala13 < 0.15 Å). A Ramachandran plot for the ϕ and ψ angles for the position-average structure was made (data not shown), in which 15 pairs cluster at $-57°$ and $-47°$ whereas 5 residues have positive ψ angles.

Figure 5 shows the stereoview superimposition of N- and C-terminal capping structures of NPT. At the N-terminus (Fig. 5a), a side chain–side chain hydrophobic interaction between Met2 and Leu7, termed the hydrophobic staple motif, was revealed. Together with the reciprocal side chain and backbone H bonds between Glu6 and Ser3,[22] the hydrophobic side chain contact further stabilizes the terminus. The peptide backbone amide of Asn18 bonds with the CO of Lys15, forming a 3_{10} structure; this bond also bifurcates to include H-bonding with CO of Phe14. The side chain of Asn18 H-bonds to the main chain CO of Phe14 at the C-terminus (Figure 5b), consistent with the NOE connectivities in NMR studies.[27] This H-bonding pattern is present in all 10 solution structures of NPT.

Discussion

The length of the α helices in globular proteins on average is short enough so that capping interactions can exert a major influence on the stability of helices.[12,13] Motifs observed in the native state of proteins can also

Table 2 [1]H chemical shifts of assigned resonances of NPT at 10 °C

Residues	NH	$^{\alpha}$H	$^{\beta}$H	$^{\gamma}$H	$^{\delta}$H	Others	$^{3}J_{HNa}$[b]
Acetyl		1.97					
Tyr1	8.33	4.49	2.96			6.84,7.13	6.4
Met2	8.17	4.48	1.88	2.50		CH_3 2.00	5.9
Ser3	8.63	4.45	4.03,4.32				5.9
Glu4	9.03	4.10	2.11,2.15	2.40			4.3
Asp5	8.53	4.44	2.62,2.67				5.9
Glu6	8.00	4.09	2.08,2.25	2.34,2.42			5.9
Leu7	8.43	4.10	1.79	1.66	0.88		5.3
Lys8	8.25	4.12	1.93	1.67	1.72	ε-CH_2 2.97	4.7
Ala9	7.99	4.24	1.50				5.9
Ala10	8.16	4.25	1.53				6.4
Glu11	8.26	4.17	2.17	2.33			4.8
Ala12	8.03	4.10	1.51				5.9
Ala13	7.98	4.13	1.48				4.3
Phe14	8.07	4.38	3.25			7.28,7.37	5.9
Lys15	8.03	4.12	1.88	1.64	1.73	ε-CH_2 3.03	5.9
Arg16	7.82	4.17	1.85	1.70	3.22	NH 7.30	6.4
His17	8.08	4.64	3.13,3.25			7.30,8.58	8.0
Asn18	8.28	4.80	2.49,2.67			6.96,7.40	
Pro19		4.51	2.34	2.04	3.72		
Pro19′		4.50	2.34	2.04	3.71		
Thr20	8.33	4.33	4.25	1.25			6.9
Thr20′	8.51	4.33	4.25	1.28		6.93	
Amide	7.29,7.55						

[a]Chemical shifts are measured relative to internal 3-(trimethylsilyl) propionic 2,2,3,3-d_4 acid sodium salt. Peptide concentration is 4.0 mM.
[b]Coupling constants (in Hz) are corrected values for line shape effects using method by Wüthrich.[26]

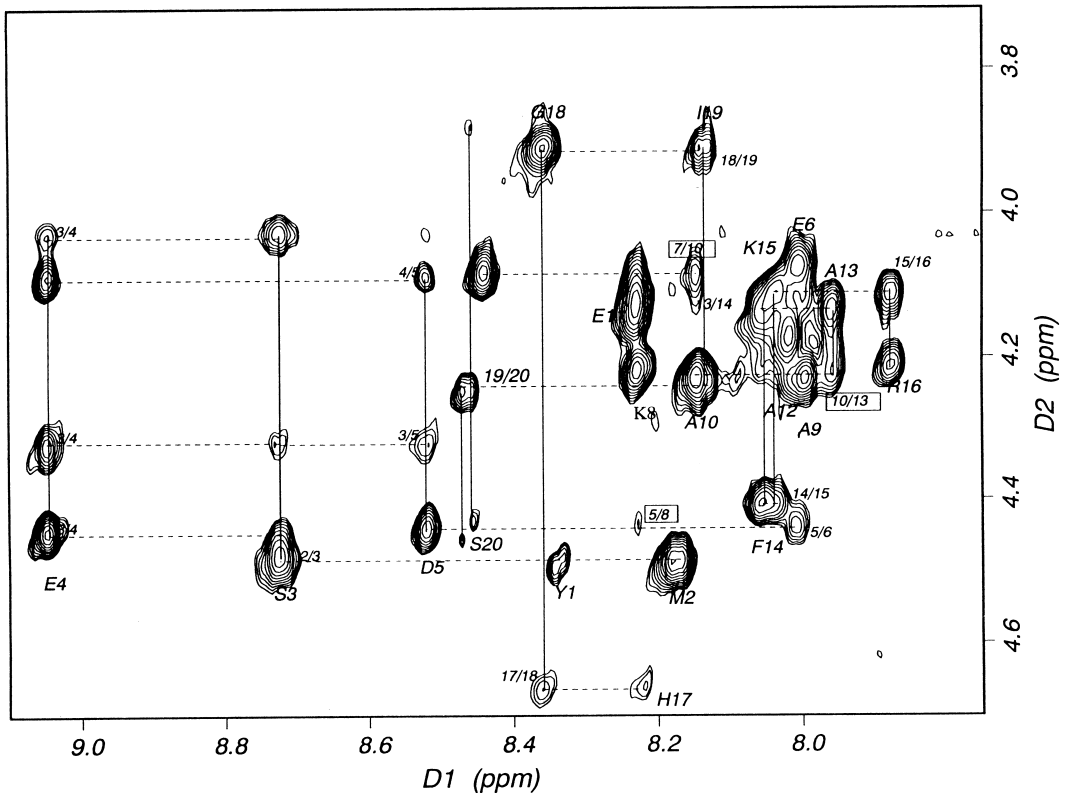

Figure 3. $^{\alpha}$H–NH region of the NOESY spectrum of FGI at 10 °C. One-letter symbols and sequential numbers in the sequence are used to identify the amino acid spin systems. The sequential and medium range cross peaks are indicated by the sequential numbers of residues.

be detected in helical peptide models,[15,17,22] and in this report, we have investigated the structure present in a series of helical peptide models containing a near consensus sequence[15] to analyze the interactions controlling the C-terminal structure of the helix.

Given the potentially crucial role of the ends in short helices, the nature and stability of the interactions responsible need to be specified. At the N-terminus, polar side chains tend to be used to replace at least part of the missing main chain bonding.[16] The N-terminal

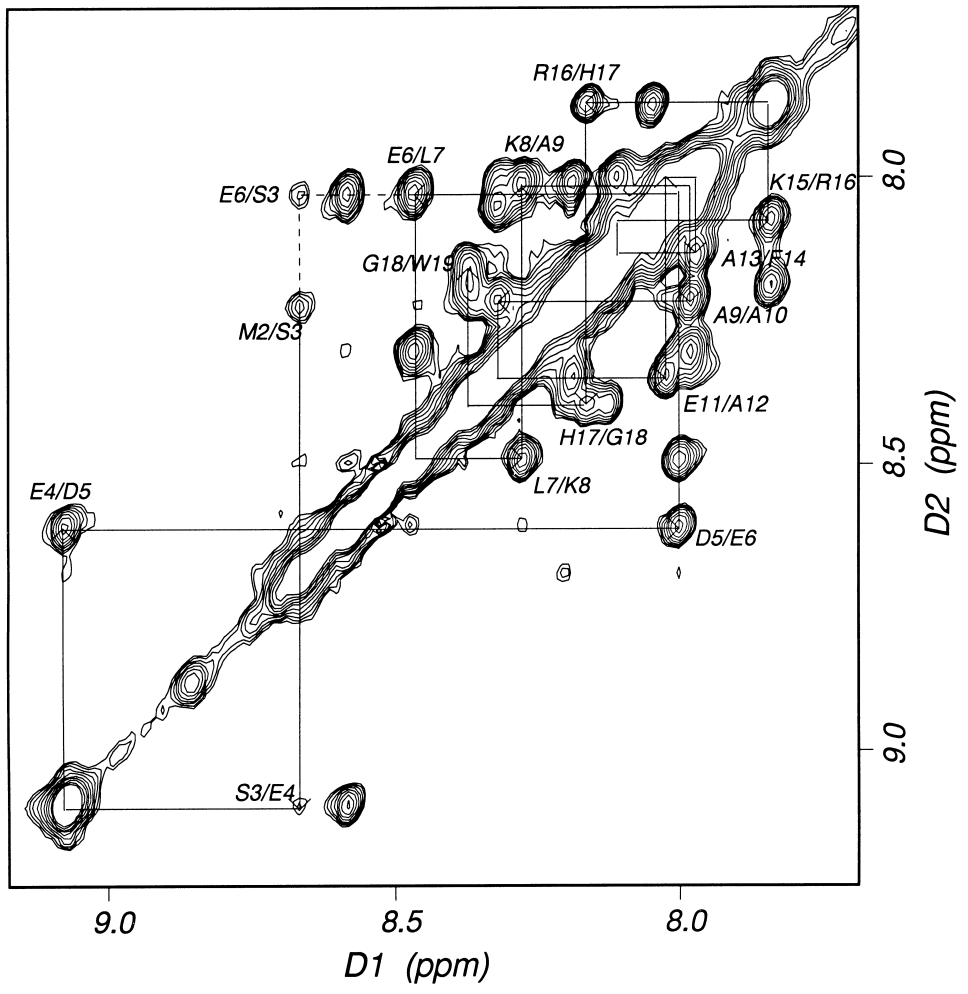

Figure 4. Amide–amide region of NOESY spectrum of peptide GWS at 10 °C in H_2O/D_2O (90/10) with mixing time, 200 ms. The cross peaks are indicated by the one-letter symbols and sequential numbers of corresponding residues. A stretch of sequential amide–amide cross peaks can be seen from Met2 to Trp19.

capping box structure described by Harper and Rose is present in all the peptides of this study, reflecting the frequency of the pattern SXXE near the N-terminus of protein helices.

This interaction involves H bonding between the side chain of Ser and the backbone NH of Glu, and reciprocal H-bonding between the Glu side chain and the main chain of Ser.[16] In addition, nonpolar side chains near the N-terminus have been implicated in stabilizing bonds in the capping motif.[11,18] The mechanism probably involves solvent interactions as well as van der Waals packing effect.[17] Helix dipolar interactions may also be involved, since negative charges are helix stabilizing near the N-terminus and destabilizing at the C-terminus.[3] As can be seen in Figure 5a, the classic capping box structure forms a characteristic flattened arch across the helix axis, thereby preventing extension of the helix in the N-terminal direction.

The strategy at the C-terminus is different, although polar side chains can still participate in helix termination.[17,27] Thus a stable C-terminal structure involving Asn at the C-terminus is seen in the NPT helix (Table 1). One difference between the N- and C-termini is that the side chains point away from the C-terminus—the side chains of helical residues are inclined towards the N-terminus by about 52°.[28] This favors polar side chain–main interactions at the N-terminus, but not at the C-terminus. The Asn side chain in NPT forms a tighter 3_{10} helical structure allowing it to reach the CO of Phe 14. This is one reason that Gly is so important at the C-terminus: its ability to assume the α_L conformation allows succeeding side chains to swing into position so that they can interact with the helix. Gly readily forms 3_{10} structure, lacking the normal side chain restriction. The Gly side chain in GVP forms bifunctional main chain–main chain H-bonds with Phe 14 and Lys 15: Gly18/Phe14, Gly18/Lys15 (data not shown). The Pro20 residue enhances this structure by interacting with the aromatic ring of Phe14—an interaction reminiscent of the nonpolar interaction, which stabilizes the N-terminal capping box. Prieto and Serrano[29] in fact have suggested that Pro may be involved as a C-capping element in general, from a statistical sequence comparison.

The sampling of different C-terminal structures analyzed in this work is insufficient to allow us to determine

Table 3 Summary of constraints used in the simulated annealing and structure statistics of the 10 solution structures of peptide NPT

NOEs			102
	Intraresidue	47	
	Sequential	37	
	Medium	18	
Dihedral angles			18
Total number of constraints			120(6/residue)
Total energy (kcal/mol)			96.3 ± 4.0
	Bonds	57.9 ± 4.0	
	Angles	109.8 ± 2.1	
	Dihedrals	20.2 ± 1.4	
	Improper	1.03 ± 0.11	
	Non-bond energy	97.4 ± 2.9	
	Coulomb energy	-190.0 ± 3.0	
Penalty energy (kcal mol^{-1})			3.30 ± 0.48
	Distance	2.78 ± 0.41	
	Dihedral angle	0.52 ± 0.12	
NOE restraint violation[b]			
	Number (>0.1 Å)		4.4 (3–6)
	Sum (Å)		0.97 (0.86–1.12)
	Maximum (Å)		0.17 (0.13–0.21)

[a]Energies are calculated using the CVFF forcefield in INSIGHT II (Biosym Technologies, Inc.).
[b]Average among the 10 solution structures and range (in parentheses).

why Schellman motif structures are less stable than the alternative. Obvious factors would include entropy, dipolar effects, and packing of neighboring side chains. Competition with the normal helix pattern has always to be taken into account in terminating chains at either end.[21] That is a terminal structure competes with the tendency of the helix to elongate. Thus at the N-terminus capping boxes overcome helix extension by multiple H-bonding interactions, including solvent as well as intramolecular interactions. In general, C-terminal structure appears to be less stabilizing than N-terminal structures, as seen in the asymmetric distribution of the helical structure in many of the peptide models studied to date. The basis for this needs to be established using detailed comparative studies of the structure present, rather than relying on CD comparisons which cannot resolve the specific interactions that are involved.

Experimental

Peptide synthesis and purification

All peptides were synthesized on a MilliGen/Biosearch 9600 automated synthesizer using PAL resin (from Milligen/Biosearch, Massachusetts) and Fmoc chemistry with BOP and HOBt as coupling reagents. N-terminal acetylation was achieved by reacting the peptide-linked resin with acetyl anhydride solution. The crude product was purified by reverse phase HPLC (Econosil C-18 RP 250×22.5 mm) as described previously,[30] and the purity was checked on a Waters analytical column (Delta Pak C18, 300×3.9 mm). The correct molecular weight of the peptide was verified by electrospray ionization mass spectroscopy, using a Vestec Model 201 mass spectrometer.

Circular dichroism spectra

CD spectra were recorded on an Aviv DS60 spectropolarimeter equipped with a HP 89100A temperature controller. The wavelength of the instrument was calibrated with (+)-10-camphorsulfonic acid.[31] The peptide concentration was determined by the tyrosine UV absorption with $\varepsilon = 1{,}450\ M^{-1}\,cm^{-1}$ at 275.5 nm, 25 °C in 6.0 M GnHCl.[32] ε = (number of Trp)×5500 + (number of Tyr)×1490 $M^{-1}\,cm^{-1}$ at 280 nm was used to calculate the concentration of the peptide containing Tyr and Trp residues. CD measurements were performed in 10 mM KF solutions in a 1 mm pathlength cell at a peptide concentration of ca. 30 mM, pH 6.0, 4 °C, averaging three scans with a step size of 0.5 nm for the spectra shown.

NMR spectroscopy

All NMR samples were prepared by dissolving lyophilized peptides in distilled H_2O or D_2O to certain peptide concentrations. The H_2O samples also contained 10% D_2O for locking and 0.25 mM of the sodium salt of 3-(trimethylsilyl)-[3,3,2,2,-D] propionic acid, which served as an internal chemical shift reference. The pH value was adjusted using a small amount of concentrated sodium hydroxide solution until the pH meter reading was 5.0.

^{1}H NMR spectra were acquired on a Varian UNITY 500 spectrometer. Two-dimensional spectra were collected in the pure absorption mode according to the method of States et al.[33] Sets of standard TOCSY[34] with mixing times of 50 and 98 ms, DQF-COSY,[35] NOESY[36–38] with mixing times of 150, and 300 ms and ROESY[39] spectra with a mixing time of 50 ms were accumulated at 0, 10, 25 °C at pH 5.0. Each 2-D data set contained 512 FIDs with 2K complex data points each, obtained by collecting 32 or 48 added free induction decays after 4 dummy scans. Spectra were Fourier transformed in both t1 and t2 dimensions after apodization with a skewed sine bell function, typically with a 60° phase shift and skew of 0.6. All NMR data were processed on a Silicon Graphics CRIMSON workstation using the FELIX 2.3 software (Biosym Technologies Inc.).

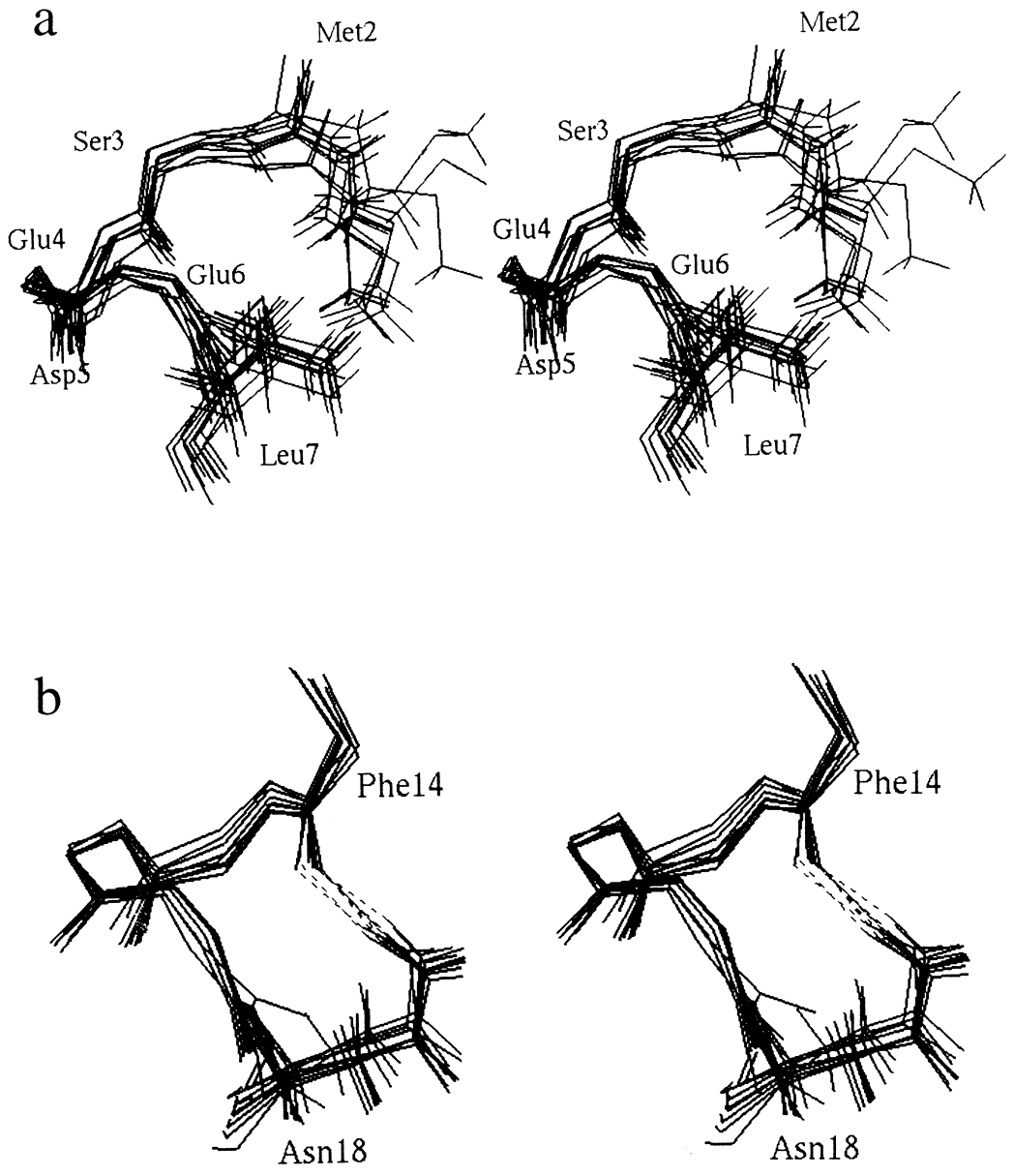

Figure 5. Hydrophobic staple motif, SXXE capping and asparagine capping structures of NPT: (a) The hydrophobic staple forms between Met2 and Leu7 residues and enhances the capping box of Ser3Glu4Asp5Glu6. The superimposition is made by minimizing the RMSD of C′, C^{α} and N from residues Met2 to Leu7 between the individual structure and the position-average structure; (b) The side chain of Asn18 swings back to H-bond the CO of Phe14 to stabilize the C-terminus. The superimposition was done by minimizing the RMSD of C′, C^{α} and N from residues Phe14 to Asn18 between the individual structure and the position-average structure.

Computational procedure

All NOESY cross peaks were transformed into distance limits as described by Gong et al.[17] Mechanics simulations were carried out on a Silicon Graphics CRIMSON computer using the Consistent Valence Force Filed (CVFF).[40,41] Biharmonic potential was used for dihedral angle constraints (E_{ϕ}) as for NOE distance constraints.[17] Dihedral angles constraints to $-160° < \phi < -80°$ for residues with ${}^{3}J_{HN\alpha} > 8.5$ Hz and to $-90° < \phi < -40°$ for residues with ${}^{3}J_{HN\alpha} < 5.5$ Hz were employed. Calculations were carried out in vacuo with $\varepsilon = 1$ and a net charge of zero. The cutoff radius for non-bond interactions was 9 Å, with a switching distance of 1.5 Å. The initial structures of peptides were modeled as extended chains using the INSIGHT II program.

Acknowledgements

This research was supported by grants from the NIH (GM 40746) and the Human Frontiers of Science Program.

References

1. Pauling, L.; Corey, R. B.; Branson, H. R. *Proc. Natl. Acad. Sci. USA* **1951**, *37*, 205.
2. Levitt, M. *Biochemistry* **1978**, *17*, 4277.
3. Kallenbach, N. R.; Lyu, P. C.; Zhou, H. X. In *Circular Dichroism and the Conformational Analysis of Biomolecules*;

Fasman, G. D., Ed.; Plenum Press: New York, 1996; pp 201–259.
4. Zimm, B. H.; Bragg, J. K. *J. Chem. Phys.* **1959**, *31*, 526.
5. Poland, D. C.; Sheraga, H. A. *Theory of Helix–Coil Transitions in Biopolymers*; Academic Press: New York, 1970.
6. Scheraga, H. A. *Pure Appl. Chem.* **1978**, *50*, 315.
7. Creamer, T. P.; Rose, G. D. *Proc. Natl. Acad. Sci. USA* **1992**, *89*, 5937.
8. Hol, W. G. J. *Prog. Biophys. Mol. Biol.* **1985**, *45*, 149.
9. Lockhardt, D. J.; Kim, P. S. *Science* **1993**, *260*, 198.
10. Padmanabhan, S.; Baldwin, R. L. *Protein Sci.* **1994**, *3*, 1992.
11. Creamer, T. P.; Rose, G. D. *Protein Sci.* **1995**, *4*, 1305.
12. Richardson, J. S.; Richardson, D. C. *Science* **1988**, *240*, 1648.
13. Presta, L.; Rose, G. D. *Science* **1988**, *240*, 1648.
14. Serrano, L.; Fersht, A. R. *Nature* **1989**, *342*, 296.
15. Lyu, P. C.; Zhou, H. X.; Jelveh, N.; Wemmer, D. E.; Kallenbach, N. R. *J. Am. Chem. Soc.* **1992**, *114*, 6560.
16. Harper, E. T.; Rose, G. D. *Biochemistry* **1993**, *32*, 7605.
17. Gong, Y.; Zhou, H. X.; Guo, M.; Kallenbach, N. R. *Protein Sci.* **1995**, *4*, 1446.
18. Munoz, V.; Blanco, F.; Serrano, L. *Nature Struct. Biol.* **1995**, *2*, 380.
19. Watson, H. C. *Prog. Stereochem.* **1969**, *4*, 299.
20. Schellman, C. In *Protein Folding*; Jaenicke, R., Ed.; Elsevier/North Holland Biomedical Press: Amsterdam, 1980; pp 53–61.
21. Aurora, R.; Srinivasan, R.; Rose, G. D. *Science* **1994**, *264*, 1126.
22. Lyu, P. C.; Wemmer, D. E.; Zhou, H. X.; Pinker, R. J.; Kallenbach, N. R. *Biochemistry* **1993**, *32*, 421.
23. Gans, P. J.; Lyu, P. C.; Manning, M. C.; Woody, R. W.; Kallenbach, N. R., *Biopolymers* **1991**, *31*, 1605.
24. Woody, R. W. In *The Peptides*; Gross, E.; Meienhofer, J., Eds.; Academic Press: New York, 1985; Vol. 7, pp 15–114.
25. Charkrabarthy, A.; Kortemme, T.; Baldwin, R. L. *Protein Sci.* **1994**, *3*, 843.
26. Wüthrich, K. *NMR of Proteins and Nucleic Acids*; John Wiley & Sons: New York, 1986.
27. Zhou, H. X.; Lyu, P. C.; Wemmer, D. E.; Kallenbach, N. R. *J. Am. Chem. Soc.* **1994**, *116*, 1139.
28. Schneider, J. P.; DeGrado, W. F. *J. Am. Chem. Soc.* **1998** (in press).
29. Prieto, J.; Serrano, L. *J. Mol. Biol.* **1997**, *274*, 276.
30. Lyu, P. C.; Liff, M. I.; Marky, L. A.; Kallenbach, N. R. *Science* **1990**, *250*, 669.
31. Chen, G. C.; Yang, J. T. *Anal. Lett.* **1977**, *10*, 1195.
32. Brandts, J. F.; Kaplan, L. J. *Biochemistry* **1973**, *12*, 2011.
33. States, D. J.; Haberkorn, R. A.; Ruben, D. J. *J. Magn. Reson.* **1982**, *48*, 286.
34. Bax, A.; Davis, G. *J. Magn. Reson.* **1985**, *65*, 355.
35. Rance, M.; Sorensen, O. W.; Bodenhausen, G.; Wagner, G.; Ernst, R. R.; Wüthrich, K. *Biochem. Biophys. Res. Commun.* **1983**, *117*, 479.
36. Jeener, J.; Meier, B. H.; Bachmann, P.; Ernst, R. R. *J. Chem. Phys.* **1979**, *71*, 4546.
37. Kumar, A.; Ernst, R. R.; Wüthrich, K. *Biochem. Biophys. Res. Commun.* **1980**, *95*, 1.
38. Wider, G.; Macura, S.; Kumar, A.; Ernst, R. R.; Wüthrich, K. *J. Magn. Reson.* **1984**, *56*, 207.
39. Bax, A.; Davis, G. *J. Magn. Reson.* **1985**, *63*, 207.
40. Maple, J. R.; Dinur, U.; Hagler, A. T. *Proc. Natl. Acad. Sci. USA* **1988**, *85*, 5350.
41. Dauber-Osguthorpe, P.; Roberts, V. A.; Osguthorpe, D. J.; Wolff, J.; Genest, M.; Hagler, A. T. *Proteins: Struct. Funct. Genet.* **1988**, *4*, 31.